Available online at www.sciencedirect.com
SCIENCE DIRECT®
Journal of Sound and Vibration 264 (2003) 1167–1186
JOURNAL OF SOUND AND VIBRATION
www.elsevier.com/locate/jsvi

Fundamental natural frequencies of thin cylindrical shells: a comparative study

M. El-Mously*

C.E. Department (258), University of Nevada at Reno, Reno, NV 89557, USA

Received 20 March 2002; accepted 1 September 2002

Abstract

A comparative study of three approximate "explicit" formulae for estimating the fundamental natural frequency of a thin cylindrical shell, and its associated fundamental modenumber is presented. The objective is to identify the limits of the validity of each formula. The three approximate formulae considered in this study are based on: (a) the Weingarten–Soedel approximation of the Donnell–Mushtari–Vlasov equations, (b) the Calladine–Koga improved classical-beam-on-Winkler-foundation model, and (c) the Timoshenko-beam-on-Pasternak-foundation analogy of the shell. Results are compared against the analytical solutions of the equations of motion of Flügge, and results obtained by a commercial finite-element package. Tabulated results are given for length-to-radius ratios of 1, 2, 5, 10, and 20, and radius-to-thickness ratios of 20, 50, 100, 200, and 500.

1. Introduction

In 1888, Love [1] presented his seminal paper on the free vibration of thin shells; this paper laid the foundation of the modern understanding of shell structures. Much effort has been made on improving on Love's theory, resulting in numerous theories in the literature: see Leissa [2] for a comprehensive review on the subject. Koiter [3], however, showed that differences among these theories are of the same order of magnitude as the error inherent in the Love–Kirchhoff hypothesis.

Analytical analyses have been investigated by several authors. Methods of analyses vary from the direct solution of the governing equations: see, e.g., Refs. [4,5]; the variational and energy

*Corresponding author. California Department of Transportation, Division of Structures Design, 1801 30th Street MS 9-4/11G, Sacramento, CA 95816, USA. Tel.: +1-775-784-4215; fax: +1-775-784-1390.
E-mail address: mohey_el-mously@dot.ca.gov (M. El-Mously).

0022-460X/03/$ - see front matter
doi:10.1016/S0022-460X(02)01391-3

methods: see, e.g., Refs. [6,7]; the finite-element method, see, e.g., Ref. [8]; and the approximate analytical methods: see, e.g., Refs. [9–14].

Closed-form expressions based on the direct solution of the governing equations are available in the literature only for shells having their edges constrained to remain circular but unrestrained axially [2]. These expressions afford a valuable insight into the shell behavior and its sensitivity to changes in any of the system parameters. Several attempts have been devoted to derive approximate explicit expressions for the fundamental natural frequency of cylindrical shells having other types of edge restraints: see, e.g., Ref. [2]. Among the widely used approximation in the literature is that of Yu [9], who showed that the characteristic equation of a cylindrical shell whose circumferential wavelength of deformation is negligibly small compared to the axial one, is similar to the characteristic equation for the lateral vibration of an analogous Bernoulli–Euler beam. Weingarten [10] utilized the Donnell–Mushtari–Vlasov (DMV) theory with the contribution of in-plane inertia neglected. He showed that by using Yu's approximation [9], the characteristic roots of the DMV theory become similar to those of freely vibrating Bernoulli–Euler beams. This has enabled him to derive an approximate formula for the natural frequency of cylindrical shells. Soedel [11] used the Galerkin method with the DMV theory, and a single set of beam functions to derive an explicit expression for the natural frequency of cylindrical shells. By approximating a number of insignificant terms, Soedel [11] obtained a formula identical to that given by Weingarten [10]. Koga [13] used an asymptotic expansion of the characteristic roots of the Budiansky equations to derive an explicit formula for the natural frequency of cylindrical shells. His formula is identical to that given by Calladine [12], which is based on the approximation of Yu [9].

In a previous paper [14], it was shown that for a particular regime of behavior of the shell, where the contributions of circumferential stretching and longitudinal bending to the strain energy are negligibly small, the Lagrangian of the shell simplifies to that of a Timoshenko beam mounted on Pasternak foundation (TP). This has enabled in deriving explicit formulae for the fundamental natural frequency of the shell and its associated fundamental modenumber.

The three "approximate" explicit formulae mentioned above are valid only within the limitations of their hypothesis. The limits on the validity of those formulae can be identified through a systematic comparison against the "exact" solution. In the case of freely vibrating cylindrical shells, "exact" solutions are available in the literature often in graphical forms. Investigators, therefore, validate their approximate analyses through comparisons with scattered examples in the literature, which might fall within the limits of the validity of their hypothesis: see, e.g., Ref. [14].

The main aim of the present paper is to investigate the limits of the validity of each of the three approximate models mentioned above. The work begins with a brief description of the equations of motion of the shell, derived by Flügge [15]. Next, the three approximate models are briefly presented. A map identifying the different regimes of the shell behavior is then constructed. Finally, comparative studies between the three approximate models against the exact analytical solutions as well as the finite-element results are presented. Throughout the paper, the small-displacement theory is assumed. The material considered is assumed homogenous, linearly elastic, and isotropic.

2. Methods of analysis

2.1. Exact analysis

Fig. 1 shows a thin-walled right circular cylindrical shell of axial length L, mean radius a, and uniform wall thickness t; a list of symbols is given in the nomenclature. The present analysis is based on the theory of Flügge [15], where terms of the order $O(t/a)^4$ and higher are discarded in comparison to unity. These equations are given by

$$L_1(u) + L_4(v) + L_5(w) = 0, \quad L_4(u) + L_2(v) + L_6(w) = 0, \quad L_5(u) + L_6(v) + L_3(w) = 0, \tag{1}$$

where the partial differential operators $L_1, L_2, \ldots, L_6$ are given by

$$\begin{aligned}
L_1 &= a\frac{\partial^2}{\partial x^2} + \frac{1-\nu}{2a}\left(1 + \frac{t^2}{12a^2}\right)\frac{\partial^2}{\partial\theta^2} - \frac{\rho a(1-\nu^2)}{E}\frac{\partial^2}{\partial\tau^2},\\
L_2 &= \frac{1}{a}\frac{\partial^2}{\partial\theta^2} + \frac{a(1-\nu)}{2}\frac{\partial^2}{\partial x^2} + \frac{3a(1-\nu)}{2}\frac{t^2}{12a^2}\frac{\partial^2}{\partial x^2} - \frac{\rho a(1-\nu^2)}{E}\frac{\partial^2}{\partial\tau^2},\\
L_3 &= \frac{1}{a} + \frac{t^2}{12a^2}\left(a^3\frac{\partial^4}{\partial x^4} + 2a\frac{\partial^4}{\partial x^2\,\partial\theta^2} + \frac{1}{a}\frac{\partial^4}{\partial\theta^4} + \frac{2}{a}\frac{\partial^2}{\partial\theta^2} + \frac{1}{a}\right) + \frac{\rho a(1-\nu^2)}{E}\frac{\partial^2}{\partial\tau^2},\\
L_4 &= \frac{1+\nu}{2}\frac{\partial^2}{\partial x\,\partial\theta}, \quad L_5 = \nu\frac{\partial}{\partial x} - \frac{t^2}{12a^2}\left(a^2\frac{\partial^3}{\partial x^3} - \frac{1-\nu}{2}\frac{\partial^3}{\partial x\,\partial\theta^2}\right),\\
L_6 &= \frac{1}{a}\frac{\partial}{\partial\theta} - \frac{a(3-\nu)}{2}\frac{t^2}{12a^2}\frac{\partial^3}{\partial x^2\,\partial\theta}.
\end{aligned} \tag{2}$$

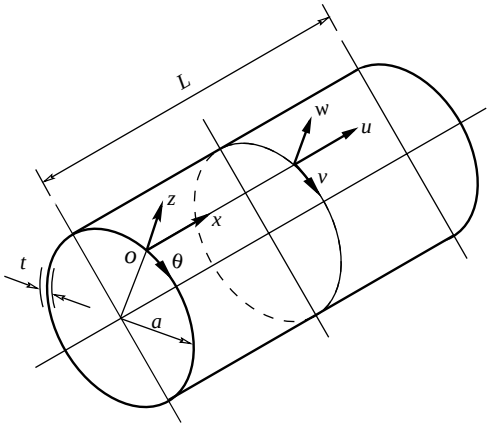

Fig. 1. Cylindrical shell showing an x, θ, z co-ordinate system and the components of small deformation in the x, θ and z directions.

Eq. (1) must satisfy the following boundary conditions (four at each edge):

$$\begin{aligned}
&(u)=0 \quad \text{or} \quad \left(\frac{\partial u}{\partial x}+\frac{v}{a}\left(\frac{\partial v}{\partial \theta}+w\right)-\frac{t^2}{12a}\frac{\partial^2 w}{\partial x^2}\right)=0,\\
&(v)=0 \quad \text{or} \quad \left(\frac{1}{a}\frac{\partial u}{\partial \theta}+\frac{\partial v}{\partial x}+\frac{t^2}{4a^2}\left(\frac{\partial v}{\partial x}-\frac{\partial^2 w}{\partial x\,\partial \theta}\right)\right)=0,\\
&(w)=0 \quad \text{or} \quad \left(\frac{\partial^3 w}{\partial x^3}-\frac{1}{a}\frac{\partial^2 u}{\partial x^2}-\frac{(3-\nu)}{2a^2}\frac{\partial^2 v}{\partial x\,\partial \theta}+\frac{(2-\nu)}{a^2}\frac{\partial^3 w}{\partial x\,\partial \theta^2}+\frac{(1-\nu)}{2a^3}\frac{\partial^2 u}{\partial \theta^2}\right)=0,\\
&\left(\frac{\partial w}{\partial x}\right)=0 \quad \text{or} \quad \left(\frac{\partial^2 w}{\partial x^2}-\frac{\nu}{a^2}\left(\frac{\partial v}{\partial \theta}-\frac{\partial^2 w}{\partial \theta^2}\right)-\frac{1}{a}\frac{\partial u}{\partial x}\right)=0.
\end{aligned} \tag{3}$$

Following Forsberg [4], the axial, u, tangential, v, and radial, w, components of deformation of a point on the shell middle-surface can be expressed as

$$u=\sum_{j=1}^{8} U_j \cos(n\theta)\, e^{\alpha_j x/a} e^{i\omega\tau}, \quad v=\sum_{j=1}^{8} V_j \sin(n\theta)\, e^{\alpha_j x/a} e^{i\omega\tau}, \quad w=\sum_{j=1}^{8} W_j \cos(n\theta)\, e^{\alpha_j x/a} e^{i\omega\tau}, \tag{4}$$

where U_j, V_j, and W_j are complex constants that can be expressed in terms of W_j using Eq. (1). Substituting Eq. (4) into Eq. (1) results in a bi-quartic algebraic equation for α^2, whose roots determine the axial dependence of the mode shapes. Satisfaction of the boundary conditions (BC), leads to a system of eight equations in terms of eight unknown constants (referred to in this paper as the BC equations). The frequency equation of the shell is obtained by setting to zero the determinant of the eight-by-eight BC coefficient matrix.

2.2. Finite-element analysis

In the present study, the commercial finite-element package SAP 2000 has been utilized. The shell was modelled by 5000 four-node quadrilateral shell elements, with 100 elements along the circumference and 50 elements along the meridian. On the basis of a preliminary convergence study, the above discretization is adequate for the present purposes.

2.3. Weingarten–Soedel expression

Both Weingarten [10] and Soedel [11] used the DMV equation:

$$D\nabla^8 w+(Et/a^2)w''''+\rho t\omega^2\nabla^4 w=0. \tag{5}$$

Postulating the fundamental solution $w=W\cos(n\theta)e^{\beta x/L}\,e^{i\omega\tau}$ into Eq. (5) results in

$$\Omega^2=(1-\nu^2)\left[1+\left(\frac{\beta a}{nL}\right)^2\right]^{-2}\left(\frac{\beta^4}{n^4\Lambda^4}\right)+\left[1+\left(\frac{\beta a}{nL}\right)^2\right]^2\left(\frac{n^4}{12}\right). \tag{6}$$

Eq. (6) is an eighth order algebraic equation for β. For H/H cylindrical shells, Eq. (6) is the exact solution of Eq. (5), with $\beta=\pi$ corresponding to the lowest axial mode. For other types of edge restraints, Weingarten [10] obtained the corresponding values of β from the asymptotic solution of Eq. (6) when $(\beta a/nL)\ll 1$, where Eq. (6) reduces to a fourth order equation, whose

characteristic roots are similar to those of a Bernoulli–Euler beam with analogous end restraints. Weingarten [10] assumed that the asymptotic values of β are constant throughout the entire domain of shell geometries.

Soedel [11] used the Galerkin method with Eq. (5), and a single set of beam functions to derive the following expression for the natural frequency of cylindrical shells:

$$\Omega^2 = \frac{\dfrac{\beta^4 a^2}{L^4 t^2}(1-\nu^2) + \dfrac{a^4}{12}\left(\dfrac{\beta^8}{L^8} + 4R\dfrac{\beta^6}{L^6}\dfrac{n^2}{a^2} + 6\dfrac{\beta^4}{L^4}\dfrac{n^4}{a^4} + 4R\dfrac{\beta^2}{L^2}\dfrac{n^6}{a^6} + \dfrac{n^8}{a^8}\right)}{\left(\dfrac{\beta^4}{L^4} + 2R\dfrac{\beta^2}{L^2}\dfrac{n^2}{a^2} + \dfrac{n^4}{a^4}\right)}, \tag{7}$$

$$R = -\frac{L^2}{\beta^2}\left(\int_0^L yy''\,\mathrm{d}x \Big/ \int_0^L y^2\,\mathrm{d}x\right). \tag{8}$$

For C/C, C/H, C/F, and H/H cylindrical shells, R is equal to 0.5499, 0.7467, –0.2441, and 1, respectively. Soedel [11] assumed a single value of $R = 1$ for all types of edge restraints, which reduces Eq. (7) to Eq. (6) of Weingarten [10].

2.4. Long-wave (LW) and short-wave (SW) expressions [16]

For values of $(\beta a/nL) \ll 1$ (Yu's LW approximation [9]), Eq. (6) reduces to

$$\Omega^2 = (1-\nu^2)\left(\frac{\beta^4}{n^4\Lambda^4}\right) + \left(\frac{n^4}{12}\right), \tag{9}$$

whereas, for values of $(\beta a/nL) \gg 1$ (SW approximation), Eq. (6) reduces to

$$\Delta^2 = (1-\nu^2) + \left(\frac{1}{12}\right)\left(\frac{\beta}{\lambda}\right)^4. \tag{10}$$

Eqs. (9) and (10) are similar (in form) to the expression for the natural frequency of a Bernoulli–Euler beam mounted on Winkler foundation. In Eq. (9), the beam and foundation actions correspond to longitudinal stretching and circumferential bending, respectively, and the appropriate non-dimensional frequency and length parameters are $\Omega = \omega(a^2/t)(\rho(1-\nu^2)/E)^{1/2}$ and $\Lambda = Lt^{1/2}/a^{3/2}$, respectively, whereas in Eq. (10), the beam and foundation actions correspond to longitudinal bending and circumferential stretching, respectively, and the appropriate non-dimensional frequency and length parameters are $\Delta = \omega a(\rho(1-\nu^2)/E)^{1/2}$ and $\lambda = L/(at)^{1/2}$, respectively.

Koga [13] used an asymptotic expansion for the characteristic roots of the equations of motion of Budiansky. He showed that the eighth order characteristic equation of the shell has two sets of four roots. One set represents the global solution that varies gradually over the shell, whereas the other represents the edge-zone solutions that decay out rapidly away from the edges. Moreover, when the shell length is not much smaller than its diameter, only the first set is relevant; and the natural frequency is given by

$$\Omega^2 = (1-\nu^2)\left(\frac{\beta^4}{n^4\Lambda^4}\frac{1}{\underline{(1+n^{-2})}}\right) + \left(\frac{n^4}{12}\frac{(1-n^{-2})^2}{\underline{(1+n^{-2})}}\right). \tag{11}$$

For large values of n, terms underlined in Eq. (11) are asymptotic to unity, and Eq. (11) simplifies to Eq. (9). The $(1+n^{-2})$ and $(1-n^{-2})^2$ terms appearing in Eq. (11) are equivalent to the contribution of circumferential displacement, respectively, to the kinetic energy, and to the change of circumferential curvature. Calladine [12] used this argument to improve the predictions of Eq. (9). His final formula is identical to Eq. (11).

2.5. Timoshenko-beam-on-Pasternak-foundation analogy

This model [14] is based on postulating a statically admissible straining field, obtained by setting to zero in the kinematics relationships of Love [1], the circumferential strain and the longitudinal change of curvature. The resulting expression for the Lagrangian of the shell is analogous to that of a Timoshenko beam mounted on Pasternak foundation. The natural frequency of the shell [14] is given by

$$\Omega^2 = \left[1 + \frac{2C_S}{(1-\nu)}\left(\frac{\pi a}{nL}\right)^2 \eta\right]^{-1}\left[\frac{\beta^4}{n^4\Lambda^4}\frac{1}{(1+n^{-2})}\right] + \left[1 + 2C_P(1-\nu)\left(\frac{\pi a}{nL}\right)^2\right]\left[\frac{n^4}{12}\frac{(1-n^{-2})^2}{(1+n^{-2})}\right], \quad (12)$$

where

$$C_S = \frac{L^2}{\pi^2}\int_0^L y'''^2\,\mathrm{d}x \Big/ \int_0^L y''^2\,\mathrm{d}x, \quad C_P = \frac{L^2}{\pi^2}\int_0^L y'^2\,\mathrm{d}x \Big/ \int_0^L y^2\,\mathrm{d}x,$$
$$\eta = 1 + \frac{C_P}{C_S}\left[\frac{1-\nu}{2(n^2+1)}\right] \cong 1. \quad (13)$$

Values of β, C_S, and C_P are given in Table 1. Note that setting $\eta = 1$ in Eq. (12) is equivalent to discarding the effect of rotary inertia in the analogous beam, which has a negligible effect on the natural frequency of the shell, except for $n = 1$. The fundamental modenumber $n = n^*$ that renders Ω a minimum, i.e., $\Omega = \Omega^*$, is given by

$$n^* \cong \left[\frac{12^{1/8}\beta^{1/2}}{\Lambda^{1/2}}\right] \Big/ \sqrt{1 + \left(\frac{3C_S}{(1-\nu)} + C_B(1-\nu)\right)\frac{\pi^2}{4(12)^{1/4}\beta\lambda}}. \quad (14)$$

Note that H/F and F/F cylindrical shells allow for inextensional modes of deformation, for which Eq. (14) is not valid. The fundamental modenumber for those shells is $n^* = 2$.

By Rayleigh's principle, using the exact frequency equation of the TP system results in an upper-bound estimate for the natural frequency of the shell. Eq. (12), however, does not yield an upper-bound estimate for the natural frequency of the shell, since it is based on an approximate frequency expression for the TP system derived in Ref. [17].

Table 1
Values of the constants β, C_S, and C_P for various sets of end restraints [14]

	C/C	C/F	C/H	H/H	H/F	F/F
β	4.730	1.875	3.927	π	0	0
C_S	5.014	0.471	2.759	1.	0	0
C_P	1.247	0.471	1.167	1.	$3/\pi^2$	0

3. Comparative study

Fig. 2 shows a plan view of a staircase-like diagram of the circumferential modenumber n^* associated with the fundamental mode of a H/H cylindrical shell having $v = 0.3$. Alternating shaded/blank "treads", respectively, correspond to odd/even values of n^*. Contours of the non-dimensional fundamental frequency parameters Ω^* and Δ^* are shown in Fig. 3. The results are based on the theory of Flügge, where an explicit frequency equation for the shell is obtained by setting to zero the determinant of the 8×8 BC coefficient matrix (cf. Section 2.1). Lines (not shown) having slopes –1/2 and +1/2 in the logarithmic plot correspond to the non-dimensional length parameters $\lambda = L/(at)^{1/2}$ and $\Lambda = Lt^{1/2}/a^{3/2}$, respectively.

Fig. 2 shows that the V-shape domains of n^* consist of two practically straight bands separated by a relatively short transition region. For large values of $\lambda = L/(at)^{1/2}$, towards the top-right corner of the figure, those bands are asymptotic to lines of slope +1/2, corresponding to a constant $\Lambda = Lt^{1/2}/a^{3/2}$. The corresponding contours of Ω^* in Fig. 3 are practically straight lines of slope +1/2, whereas the contours of Δ^* depict a festoon-like family of curves. Here, the shell behavior is dominated by longitudinal stretching and circumferential bending, and the LW approximation is valid. On the other hand, for small values of $\lambda = L/(at)^{1/2}$, towards the bottom-left corner of Fig. 2, the shell behavior is predominantly axi-symmetric, and the corresponding contours of Ω^* in Fig. 3 are asymptotic to straight lines of slope zero, whereas the contours of Δ^* are practically straight lines of slope +1/2. Here, the shell behavior is dominated by circumferential stretching and longitudinal bending, and the SW model is valid.

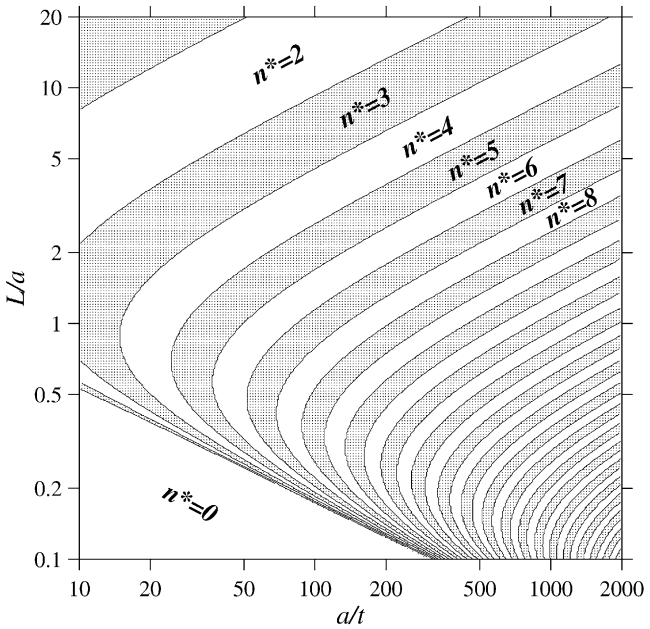

Fig. 2. A plan-view of a staircase-like diagram in relation to the circumferential modenumber n^* associated with the fundamental mode of a H/H cylindrical shell ($v = 0.3$), according to the theory of Flügge. Alternating shaded/blank "treads" correspond to odd/even values of n^*, respectively.

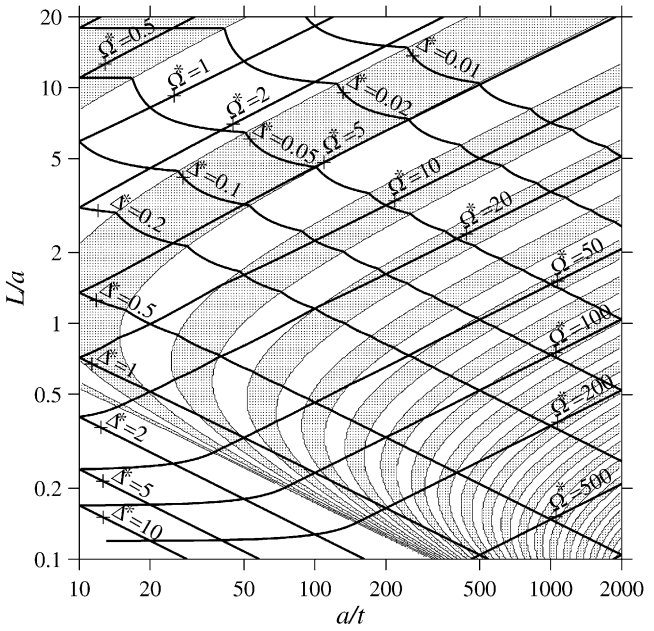

Fig. 3. Contours of the non-dimensional fundamental frequency parameters Ω^* and Λ^* for the H/H shell of Fig. 2, according to the theory of Flügge.

It is convenient at this stage to correlate the features in Figs. 2 and 3 to the WS model, Eq. (6). Assuming that n^* is continuously variable, the value of $n = n^*$ that renders the natural frequency a minimum, i.e., $\Omega = \Omega^*$, is given by

$$n^* = \frac{K\beta}{\Lambda}\sqrt{1 - \frac{\beta/K}{\lambda}}, \tag{15a}$$

which can be rearranged as

$$\left(\frac{a}{t}\right)^{1/2} = \frac{(n^*)^2}{K\beta}\left(\frac{L}{a}\right) + \frac{\beta}{K}\left(\frac{a}{L}\right), \tag{15b}$$

where $K = [12(1 - \nu^2)]^{1/4}$, with $K = 1.82$ at $\nu = 0.3$. The appearance of the L/a term in the numerator and the denominator of the two terms in the right hand side of Eq. (15b) gives rise to the V-shape curve in Fig. 2. Discarding the second term in Eq. (15b) (LW approximation) results in $n^* = (K\beta/\Lambda)^{1/2}$ ($= 2.39/\Lambda^{1/2}$ for H/H shells, $\nu = 0.3$), corresponding to lines of slope $+1/2$ in Fig. 2. On the other hand, discarding the first term in Eq. (15b) (SW approximation) results in $\lambda = \beta/K$ ($= 1.73$ for H/H shells, $\nu = 0.3$), corresponding to lines of slope $-1/2$ in Fig. 2. The points, at which the tangents to the V-shape bands are vertical, correspond to the shell proportions for which the contributions of in-plane shearing strain and twist to the strain energy of the shell are maximum. These points lie on a line of slope $-1/2$ corresponding to $\lambda = 2\beta/K$ ($= 3.46$ for H/H shells, $\nu = 0.3$).

Fig. 4 shows the boundary curves (light solid curves) of a staircase-like diagram for n^* of the H/H shell of Fig. 2 ($\nu = 0.3$), according to the theory of Flügge. The shaded "tread" corresponds

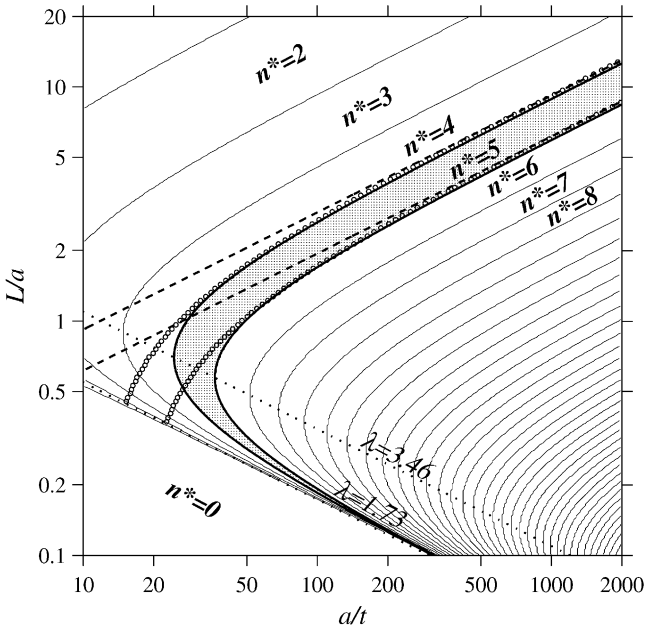

Fig. 4. A plan-view of a staircase-like diagram in relation to the circumferential modenumber n^* of a H/H cylindrical shell ($v = 0.3$). Light solid curves correspond to the boundary curves for the domains of n^* according to the theory of Flügge, with the shaded "tread" corresponding to $n^* = 5$. Bold-solid and broken curves correspond to the WS and CK predictions for $n^* = 5$, respectively, whereas open circles correspond to the TP model.

to the domain of $n^* = 5$. Bold solid and broken curves correspond to the WS and CK predictions for the boundary curves ("risers") of the domain of $n^* = 5$, whereas open circles correspond to the predictions of the TP model. The predictions of the WS model, Eq. (15), are indistinguishable from those of the Flügge theory. The predictions of the CK and TP models for n^* are in excellent agreement with the predictions of the Flügge theory for $\lambda \geqslant 40$ and $\geqslant 6$, respectively.

Fig. 5 shows contours of the percentage of relative error in the fundamental natural frequency incurred by the WS model (solid curves), the CK model (broken curves), and the TP model (open circles), using the theory of Flügge as a reference. For axi-symmetirc modes ($n^* = 0$), neither the CK model nor the TP model is applicable. On the other hand, the WS model reduces to the SW model, Eq. (10), and both are in excellent agreement with the results of the Flügge theory except for shells having $L/t \leqslant 1$. In the remainder of this paper, axi-symmetric modes of deformation will be investigated no further.

On the other hand, for asymmetric modes ($n^* \geqslant 1$), Fig. 5 shows that the predictions of the WS model are in excellent agreement with those of the Flügge theory, except for small values of n^*. Taking the 5% contour of absolute relative error as a cut-off for its validity, the WS model is valid for $n^* > 4$, corresponding to $\Lambda \leqslant 0.29$, whereas the TP predictions are in excellent agreement with those of the Flügge theory for $\lambda \geqslant 6$. The CK results, Eq. (11), are in excellent agreement with those of the Flügge theory over a wide domain of geometries, but there is no pattern for which one can set limits on the validity of the CK model, which decreases somewhat with the increase of the shell thickness.

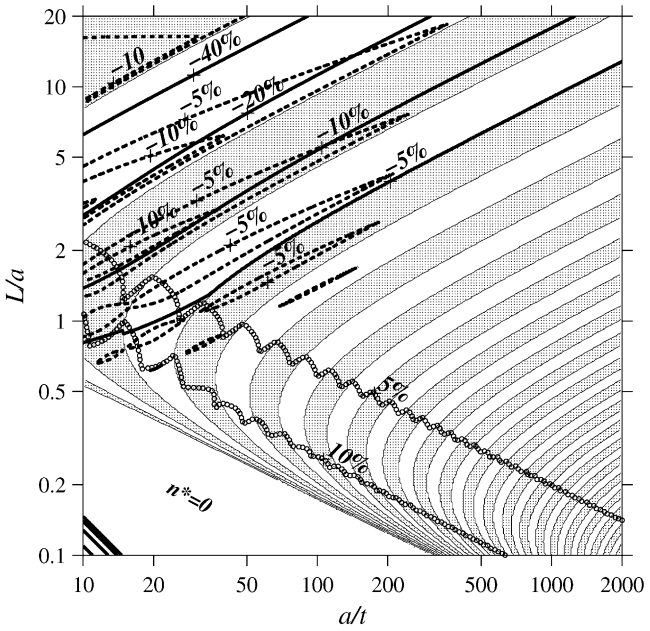

Fig. 5. Contours of the percentage of relative error incurred by the WS (solid curves), CK (broken curves), and TP (open circles) models for the H/H shell of Fig. 2: see text for details.

Figs. (6)–(11) show comparisons between the predictions of the three approximate models against the results of the Flügge theory for C/C, C/H, and C/F cylindrical shells. Figs. 6, 8 and 10 show plan-views of staircase-like diagrams of the circumferential modenumber n^* associated with the fundamental mode of C/C, C/H, and C/F cylindrical shells, respectively ($\nu = 0.3$). Alternating shaded/blank "treads", respectively, correspond to odd/even values of n^*, obtained from the theory of Flügge. Solid and broken curves, respectively, correspond to the WS and CK predictions for the boundary curves of the domains of n^*, whereas open circles correspond to the TP predictions. Figs. 7, 9 and 11 show contours of the percentage of relative error in the fundamental natural frequency incurred by the WS, CK, and TP models for C/C, C/H, and C/F cylindrical shells, respectively, using the Flügge theory as a reference. Unlike the case of H/H shells, explicit frequency equations for C/C, C/H, and C/F shells are extremely lengthy. A simple program is written to sweep along a predefined band for the natural frequency for a given value of n. The desired natural frequency is the one at which the determinant of the 8×8 BC coefficient matrix vanishes (cf. Section 2.1). By sweeping through n, both the fundamental natural frequency and its associated fundamental modenumber are obtained. The main difficulty of this approach is that the 8×8 BC coefficient matrix can become ill-conditioned due to the inclusion of hyperbolic and trigonometric terms.

The CK predictions for the fundamental natural frequency and its associated fundamental modenumber for C/C, C/H, and C/F shells, are in excellent agreement with the predictions of the Flügge theory (within 5% absolute percentage of relative error) for $\lambda \geqslant 100$, 60, and 20,

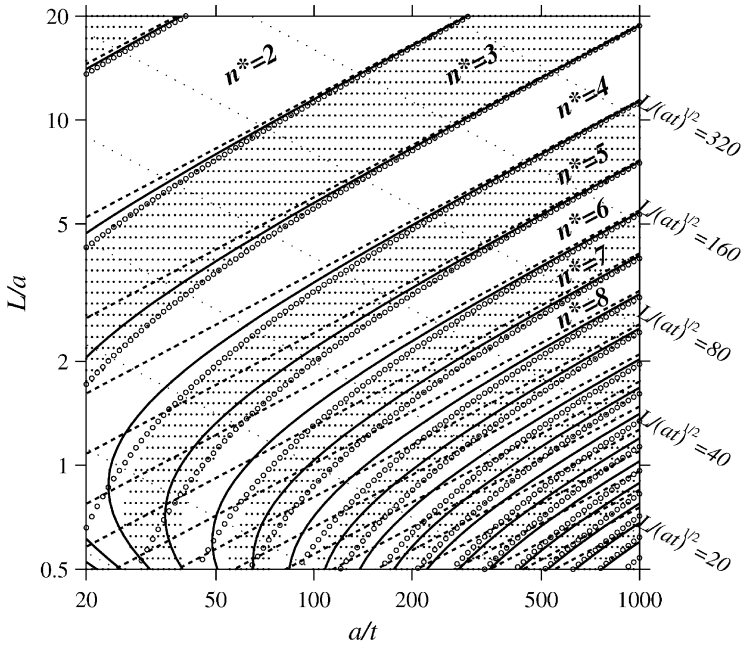

Fig. 6. A plan-view of a staircase-like diagram in relation to the circumferential modenumber n^* of a C/C cylindrical shell ($v = 0.3$). Alternating shaded/blank "treads" correspond to odd/even values of n^*, according to the theory of Flügge. Solid and broken curves correspond to the WS and CK models, respectively, and open circles correspond to the TP model.

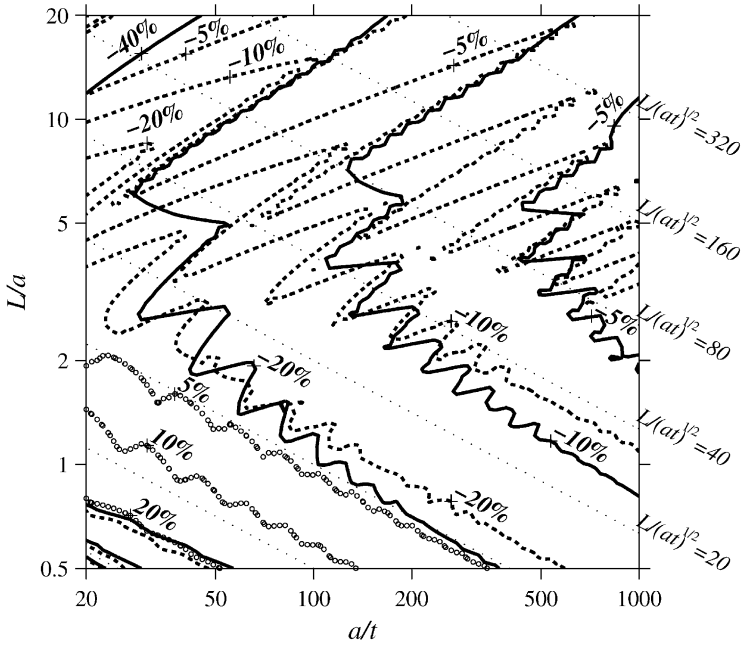

Fig. 7. Contours of the percentage of relative error incurred by the WS (solid curves), CK (broken curves), and TP (open circles) models for the C/C shell of Fig. 6: see text for details.

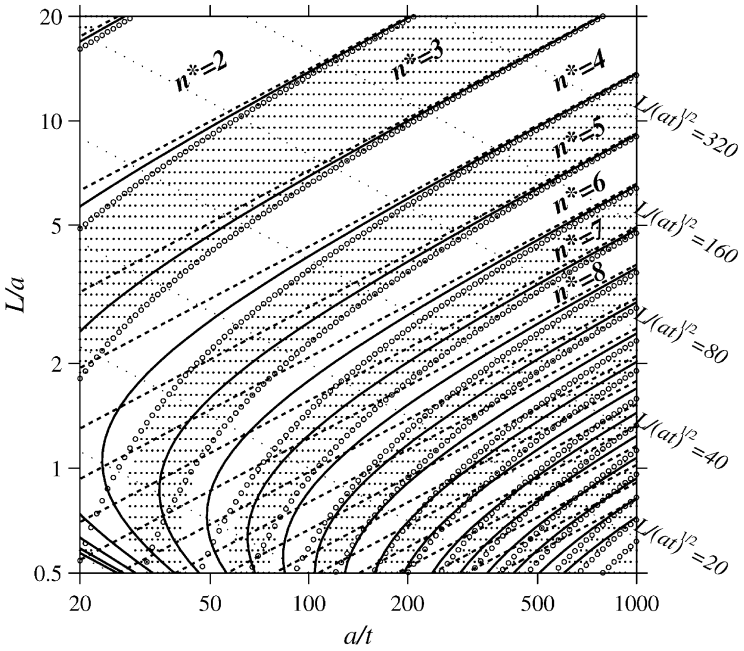

Fig. 8. A plan-view of a staircase-like diagram in relation to the circumferential modenumber n^* of a C/H cylindrical shell ($v = 0.3$). Alternating shaded/blank "treads" correspond to odd/even values of n^* according to the theory of Flügge. Solid and broken curves correspond to the WS and CK models, respectively, and open circles correspond to the TP model.

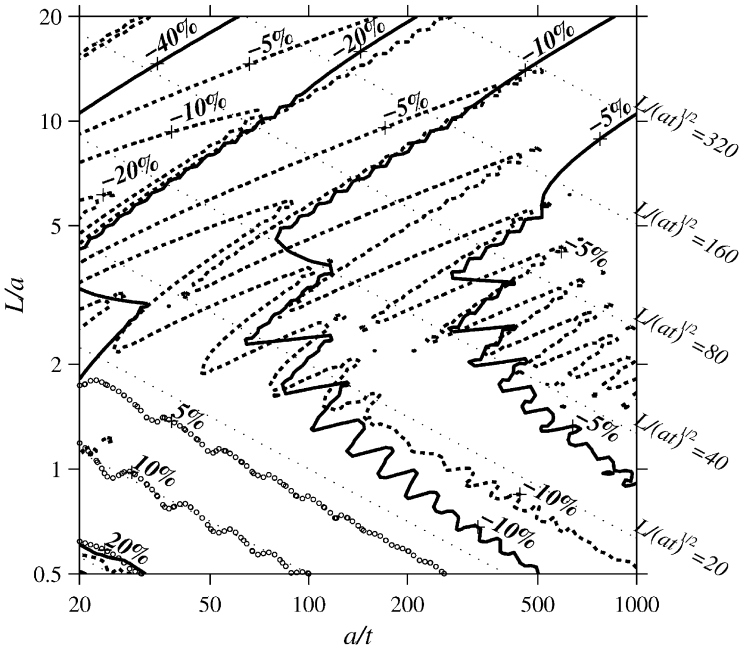

Fig. 9. Contours of the percentage of relative error incurred by the WS (solid curves), CK (broken curves), and TP (open circles) models for the C/H shell of Fig. 8: see text for details.

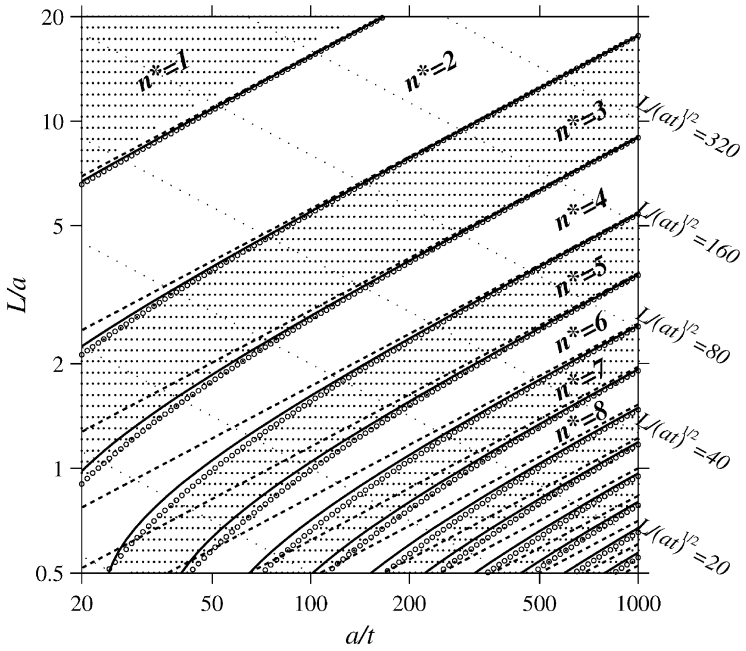

Fig. 10. A plan-view of a staircase-like diagram in relation to the circumferential modenumber n^* of a C/F cylindrical shell ($v = 0.3$). Alternating shaded/blank "treads" correspond to odd/even values of n^* according to the theory of Flügge. Solid and broken curves correspond to the WS and CK models, respectively, and open circles correspond to the TP model.

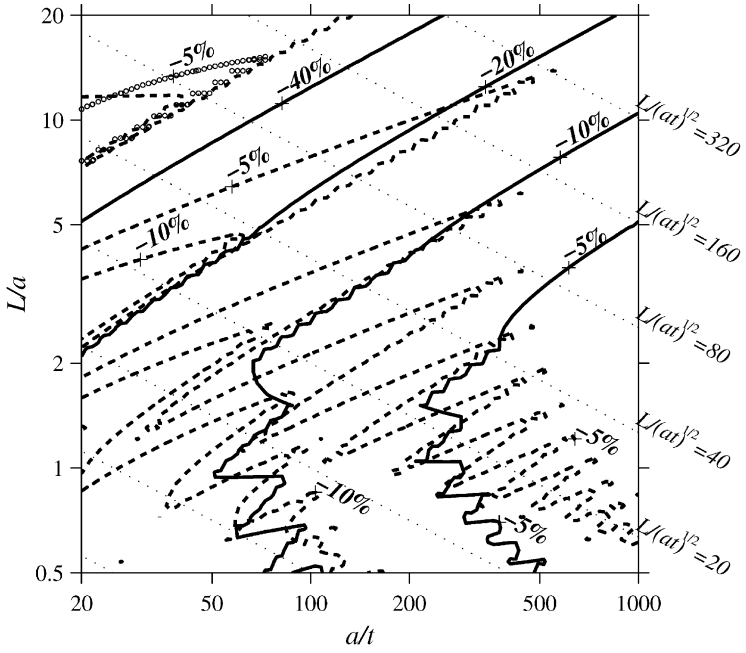

Fig. 11. Contours of the percentage of relative error incurred by the WS (solid curves), CK (broken curves), and TP (open circles) models for the C/F shell of Fig. 10: see text for details.

respectively. The wavy nature of the contours of the percentage of relative error is mainly due to the error in estimating the fundamental modenumber.

The TP model significantly extends the above limits on the validity of the CK model to about $\lambda \geqslant 10$, 8, and 2, for C/C, C/H, and C/F shells, respectively. For C/F cylindrical shells, Fig. 11 shows that the percentage of relative error incurred by the TP model for $n^* = 1$ exceeds 5% (but does not exceed 5.3%). This is mainly due to discarding the contribution of axial inertia to the kinetic energy expression in Eq. (12) (via setting $\eta = 1$).

The predictions of the WS model for n^* are in excellent agreement with the Flügge theory, except near the narrow transition zone separating the two practically straight bands of the V-shape domains of n^*, where the contributions of in-plane shearing strain and twist to the strain energy are maximum. Contours of 5% absolute relative error incurred by the WS model in predicting the fundamental natural frequency of C/C, C/H, and C/F cylindrical shells have a similar pattern. For C/C, C/H, and C/F cylindrical shells, these patterns can be depicted by $2.35\Lambda + 52.0/\lambda \leqslant 1$, $2.84\Lambda + 25.8/\lambda \leqslant 1$, and $5.93\Lambda + 10.3/\lambda \leqslant 1$, respectively. These V-shape-like cut-offs have simple interpretations. The upper branches are a direct consequence of using the DMV theory, which limits the application of the model to $n^* > 4$. The lower branches are due to approximating the true values of β, Eq. (6), by their counterparts for the Bernoulli–Euler beams, in the narrow transition zone separating the two straight bands of the domains of n^*: see Section 2.3.

Tables 2–5 show comparisons of the values of the fundamental frequency parameter Ω^* and the fundamental modenumber n^* (given between parentheses) for C/C, C/H, C/F, and H/H cylindrical shells, respectively. The results of the WS, CK, and TP models are given as percentages of relative error, using the results of the theory of Flügge as a reference. The SAP 2000 results are in excellent agreement with the results of the Flügge theory. For the four cases considered, the results of the SAP 2000 and the Flügge theory differ by less than 1%. The tabulated results confirm the earlier conclusions of this section.

As noted earlier, H/F and F/F cylindrical shells allow for inextensional modes of deformation, and for both shells the fundamental modenumber is $n^* = 2$. For H/F cylindrical shells, the inextensional frequency of the shell [14] is given by

$$\Omega^2 = \frac{n^4}{12}\frac{(1-n^{-2})^2}{(1+n^{-2})}\left[\frac{1+6(1-\nu)\,(a^2/n^2L^2)}{1+(3/(n^2+1))\,(a^2/n^2L^2)}\right]. \tag{16}$$

The corresponding expressions for the WS, CK, and TP models are given by

$$\Omega^2_{WS} = \frac{n^4}{12}, \quad \Omega^2_{CK} = \frac{n^4}{12}\frac{(1-n^{-2})^2}{(1+n^{-2})}, \quad \Omega^2_{TP} = \frac{n^4}{12}\frac{(1-n^{-2})^2}{(1+n^{-2})}\left[1+6(1-\nu)\frac{a^2}{n^2L^2}\right]. \tag{17}$$

For $n = 2$, corresponding to the fundamental mode, the absolute percentage of relative error incurred by the WS model ($\nu = 0.3$) is within 5% for $0.68 < L/a < 0.86$, whereas for $L/a < 1/4$ and > 4, the absolute percentage of relative error is asymptotic to 49.07%. On the other hand, the absolute percentage of relative error incurred by the CK and TP models is less than 5% for $L/a \geqslant 2.8$ and $\geqslant 1.2$, respectively.

Table 2
Comparison of values of the fundamental frequency parameter $\Omega^* = \omega a^2/t\sqrt{(1-\nu^2)\rho/E}$ and the fundamental modenumber n^* (given between parentheses) for C/C cylindrical shells

L/a		a/t				
		20	50	100	200	500
	Flügge	0.6574 (1)	0.9697 (2)	1.3902 (2)	2.4288 (2)	3.5337 (3)
	SAP 2000	0.6574 (1)	0.9696 (2)	1.3913 (2)	2.4327 (2)	3.5390 (3)
20	WS	−60.6% (1)	−38.5% (2)	−26.7% (2)	−18.1% (3)	−11.5% (3)
	CK	−20.3% (1)	−2.66% (2)	−5.82% (2)	−2.44% (3)	−3.94% (3)
	TP	−3.42% (1)	−1.34% (2)	−2.83% (2)	−2.19% (3)	−2.76% (3)
	$L/(at)^{1/2}$	89.44	141.4	200	282.8	447.2
	Flügge	1.1582 (2)	2.2366 (2)	3.0661 (3)	4.7741 (3)	7.5424 (4)
	SAP 2000	1.1565 (2)	2.2363 (2)	3.0667 (3)	4.7781 (3)	7.5210 (4)
10	WS	−36.7% (2)	−25.4% (2)	−15.1% (3)	−11.8% (3)	−7.06% (4)
	CK	−9.26% (2)	−11.2% (3)	−4.99% (3)	−4.75% (4)	−5.78% (4)
	TP	−0.90% (2)	−2.44% (2)	−1.57% (3)	−2.87% (3)	−2.80% (4)
	$L/(at)^{1/2}$	44.72	70.71	100	141.4	223.6
	Flügge	2.7120 (2)	4.3080 (3)	6.2774 (4)	9.2569 (5)	14.9318 (6)
	SAP 2000	2.7105 (2)	4.3081 (3)	6.2788 (4)	9.2606 (5)	14.9442 (6)
5	WS	−23.1% (3)	−20.1% (3)	−11.9% (4)	−7.68% (5)	−5.31% (6)
	CK	−6.61% (3)	−16.1% (4)	−9.32% (4)	−5.54% (5)	−5.82% (6)
	TP	+0.10% (2)	−0.73% (3)	−0.96% (4)	−1.12% (5)	−1.82% (6)
	$L/(at)^{1/2}$	22.36	35.35	50	70.71	111.8
	Flügge	6.2404 (3)	10.4686 (5)	15.3271 (6)	22.4040 (7)	36.7629 (9)
	SAP 2000	6.2376 (3)	10.4723 (5)	15.3450 (6)	22.4478 (7)	36.8545 (9)
2	WS	−27.5% (4)	−18.6% (5)	−14.6% (6)	−12.1% (7)	−7.69% (10)
	CK	−27.9% (4)	−20.1% (6)	−16.0% (7)	−11.7% (8)	−8.23% (10)
	TP	+4.77% (3)	+2.61% (5)	+1.11% (6)	+0.05% (7)	0.85% (9)
	$L/(at)^{1/2}$	8.944	14.14	20	28.28	44.72
	Flügge	12.4779 (4)	19.9836 (6)	29.1461 (7)	42.6632 (9)	70.5857 (12)
	SAP 2000	12.4650 (4)	19.9954 (6)	29.2385 (7)	42.8671 (9)	71.0883 (12)
1	WS	−25.8% (4)	−24.4% (6)	−20.4% (8)	−16.4% (10)	−11.2% (13)
	CK	−26.6% (6)	−25.3% (8)	−22.8% (9)	−18.3% (11)	−13.3% (14)
	TP	+15.4% (4)	+8.07% (6)	+4.17% (7)	+2.31% (9)	+0.64% (12)
	$L/(at)^{1/2}$	4.472	7.071	10	14.14	22.36

For F/F cylindrical shells, the predictions of the WS, CK, and TP models for the inextensional frequency of the shell are given by

$$\Omega_{WS}^2 = \frac{n^4}{12}, \quad \Omega_{CK}^2 = \Omega_{TP}^2 = \frac{n^4}{12}\frac{(1-n^{-2})^2}{(1+n^{-2})}. \tag{18}$$

The CK and TP expressions are identical to the inextensional frequency formula of Rayleigh (see Refs. [2,5]). For $n = 2$, corresponding to the fundamental mode, the WS prediction is higher than that of Rayleigh by 49.07%.

Table 3
Comparison of values of the fundamental frequency parameter $\Omega^* = \omega a^2/t\sqrt{(1-\nu^2)\rho/E}$ and the fundamental modenumber n^* (given between parentheses) for C/H cylindrical shells

L/a		a/t				
		20	50	100	200	500
	Flügge	0.4792 (1)	0.8779 (2)	1.1215 (2)	1.7903 (2)	2.9189 (3)
	SAP 2000	0.4791 (1)	0.8777 (2)	1.1217 (2)	1.7915 (2)	2.9208 (3)
20	WS	−60.5% (1)	−42.6% (2)	−31.9% (2)	−20.8% (2)	−13.3% (3)
	CK	−13.8% (1)	−0.97% (2)	−3.33% (2)	−5.56% (2)	−2.36% (3)
	TP	−4.09% (1)	−0.81% (2)	−2.23% (2)	−3.60% (2)	−1.98% (3)
	$L/(at)^{1/2}$	89.44	141.4	200	282.8	447.2
	Flügge	1.0035 (2)	1.7193 (2)	2.6766 (3)	3.7275 (3)	6.0847 (4)
	SAP 2000	1.0017 (2)	1.7185 (2)	2.6766 (3)	3.7287 (3)	6.0883 (4)
10	WS	−38.8% (2)	−24.4% (2)	−15.5% (3)	−11.6% (3)	−7.10% (4)
	CK	−3.34% (2)	−9.92% (2)	−1.92% (3)	−5.16% (3)	−3.29% (4)
	TP	−0.75% (2)	−2.60% (2)	−1.06% (3)	−2.55% (3)	−2.19% (4)
	$L/(at)^{1/2}$	44.72	70.71	100	141.4	223.6
	Flügge	2.2209 (2)	3.5742 (3)	5.4440 (4)	7.9087 (4)	12.7506 (6)
	SAP 2000	2.2180 (2)	3.5728 (3)	5.4440 (4)	7.9111 (4)	12.7560 (6)
5	WS	−29.5% (2)	−15.6% (3)	−9.52% (4)	−8.14% (4)	−4.13% (6)
	CK	−14.7% (3)	−9.67% (3)	−3.31% (4)	−5.46% (5)	−2.47% (6)
	TP	−0.43% (2)	−0.86% (3)	−0.72% (4)	−2.09% (4)	−1.29% (6)
	$L/(at)^{1/2}$	22.36	35.35	50	70.71	111.8
	Flügge	5.5090 (3)	9.3071 (4)	13.5649 (5)	19.4263 (7)	31.4708 (9)
	SAP 2000	5.5023 (3)	9.3115 (4)	13.5792 (5)	19.4422 (7)	31.5047 (9)
2	WS	−23.8% (3)	−12.7% (5)	−8.72% (6)	−6.30% (7)	−3.91% (9)
	CK	−14.1% (4)	−9.20% (5)	−7.05% (6)	−6.84% (7)	−4.72% (9)
	TP	+4.23% (3)	+1.69% (4)	+0.51% (5)	+0.01% (7)	–0.68% (9)
	$L/(at)^{1/2}$	8.944	14.14	20	28.28	44.72
	Flügge	11.0834 (4)	18.0504 (6)	25.9484 (7)	37.6447 (9)	61.3860 (12)
	SAP 2000	11.0689 (4)	18.0502 (6)	25.9961 (7)	37.7384 (9)	61.5871 (12)
1	WS	−17.6% (4)	−14.2% (6)	−13.5% (7)	−9.70% (9)	−6.15% (12)
	CK	−17.9% (6)	−15.0% (7)	−14.6% (9)	−11.1% (10)	−8.14% (13)
	TP	+12.0% (4)	+6.48% (6)	+3.66% (7)	1.97% (9)	+0.51% (12)
	$L/(at)^{1/2}$	4.472	7.071	10	14.14	22.36

4. Conclusions

On the basis of the present study, the following conclusions may be drawn:

1. A comparative study has been conducted between three approximate explicit formulae for predicting the fundamental natural frequency of vibration of a thin cylindrical shell, and its associated fundamental modenumber, taking the results of both the theory of Flügge, and the finite-element package SAP 2000, as references.

Table 4
Comparison of values of the fundamental frequency parameter $\Omega^* = \omega a^2/t\sqrt{(1-\nu^2)\rho/E}$ and the fundamental modenumber n^* (given between parentheses) for C/F cylindrical shells

L/a		a/t				
		20	50	100	200	500
	Flügge	0.1167 (1)	0.2915 (1)	0.5828 (1)	0.8609 (2)	1.2140 (2)
	SAP 2000	0.1166 (1)	0.2914 (1)	0.5828 (1)	0.8609 (2)	1.2144 (2)
20	WS	−187% (1)	−74.1% (1)	−51.1% (1)	−42.9% (2)	−28.5% (2)
	CK	−6.51% (1)	−6.62% (1)	−6.64% (1)	−0.89% (2)	−3.07% (2)
	TP	−4.80% (1)	−4.87% (1)	−4.92% (1)	−0.98% (2)	−2.89% (2)
	$L/(at)^{1/2}$	89.44	141.4	200	282.8	447.2
	Flügge	0.4448 (1)	0.8619 (2)	1.0736 (2)	1.6699 (2)	2.8123 (3)
	SAP 2000	0.4444 (1)	0.8619 (2)	1.0734 (2)	1.6697 (2)	2.8129 (3)
10	WS	−60.4% (1)	−43.5% (2)	−33.3% (2)	−21.6% (2)	−13.8% (3)
	CK	−11.8% (1)	−0.78% (2)	−2.80% (2)	−4.96% (2)	−2.03% (3)
	TP	−5.04% (1)	−1.10% (2)	−2.38% (2)	−3.77% (2)	−1.94% (3)
	$L/(at)^{1/2}$	44.72	70.71	100	141.4	223.6
	Flügge	0.9747 (2)	1.6214 (2)	2.6074 (3)	3.5347 (3)	5.8248 (4)
	SAP 2000	0.9733 (2)	1.6202 (2)	2.6078 (3)	3.5346 (3)	5.8263 (4)
5	WS	−39.5% (2)	−24.2% (2)	−15.8% (3)	−11.7% (3)	−7.19% (4)
	CK	−2.37% (2)	−8.10% (2)	−1.45% (3)	−4.30% (3)	−2.76% (4)
	TP	−1.99% (2)	−3.60% (2)	−1.57% (3)	−2.94% (3)	−2.33% (4)
	$L/(at)^{1/2}$	22.36	35.35	50	70.71	111.8
	Flügge	2.7996 (3)	4.4747 (3)	6.3852 (4)	9.3322 (5)	14.9883 (6)
	SAP 2000	2.7956 (3)	4.4734 (3)	6.3859 (4)	9.3354 (5)	14.9954 (6)
2	WS	−18.5% (3)	−14.3% (3)	−8.98% (4)	−5.97% (5)	−3.91% (6)
	CK	−2.50% (3)	−11.2% (4)	−6.28% (4)	−3.73% (5)	−4.29% (6)
	TP	−2.14% (3)	−3.25% (3)	−2.66% (4)	−2.29% (5)	−2.62% (6)
	$L/(at)^{1/2}$	8.944	14.14	20	28.28	44.72
	Flügge	5.4202 (3)	9.0514 (4)	13.1031 (5)	18.8410 (7)	30.3345 (8)
	SAP 2000	5.4147 (3)	9.0549 (4)	13.1149 (5)	18.8568 (7)	30.3815 (8)
1	WS	−19.3% (3)	−11.8% (5)	−8.51% (6)	−5.22% (7)	−3.67% (9)
	CK	−10.4% (4)	−6.94% (5)	−5.79% (6)	−4.82% (7)	−3.84% (9)
	TP	−1.83% (3)	−3.00% (4)	−3.07% (5)	−2.36% (7)	−2.61% (9)
	$L/(at)^{1/2}$	4.472	7.071	10	14.14	22.36

2. For axi-symmetirc modes ($n = 0$), neither the CK formula nor the TP formula is valid. The WS formula reduces to the SW formula, and both are valid for $\lambda = \beta/K$.
3. The WS formula is in excellent agreement with the Flügge theory (within 5% absolute relative error), for asymmetric modes of deformation ($n^* > 0$), provided that $2.35\Lambda + 52.0/\lambda \leqslant 1$, $2.84\Lambda + 25.8/\lambda \leqslant 1$, $5.93\Lambda + 10.3/\lambda \leqslant 1$, and $3.46\Lambda \leqslant 1$, for C/C, C/H, C/F, and H/H cylindrical shells, respectively.
4. The CK formula is in excellent agreement with the Flügge theory (within 5% absolute relative error) for asymmetric modes of deformation ($n^* > 0$), provided that, $\lambda \geqslant 100$, 60, and 20, for

Table 5
Comparison of values of the fundamental frequency parameter $\Omega^* = \omega a^2/t\sqrt{(1-\nu^2)\rho/E}$ and the fundamental modenumber n^* (given between parentheses) for H/H cylindrical shells

L/a		a/t				
		20	50	100	200	500
	Flügge	0.3221 (1)	0.8051 (1)	0.9382 (2)	1.3036 (2)	2.5209 (3)
	SAP 2000	0.3220 (1)	0.8049 (1)	0.9380 (2)	1.3035 (2)	2.5216 (3)
20	WS	−69.6% (1)	−47.3% (1)	−38.6% (2)	−26.5% (2)	−15.6% (3)
	CK	−8.32% (1)	−2.14% (2)	−1.36% (2)	−3.42% (2)	−1.07% (3)
	TP	−4.72% (1)	−2.42% (2)	−1.36% (2)	−2.97% (2)	−1.11% (3)
	$L/(at)^{1/2}$	89.44	141.4	200	282.8	447.2
	Flügge	0.8926 (2)	1.2950 (2)	2.1957 (2)	2.9581 (3)	5.0895 (4)
	SAP 2000	0.8909 (2)	1.2940 (2)	2.1952 (2)	2.9582 (3)	5.0908 (4)
10	WS	−42.2% (2)	−27.3% (2)	−17.7% (2)	−13.0% (3)	−7.88% (4)
	CK	+0.12% (2)	−4.11% (2)	−6.52% (2)	−2.14% (3)	−1.34% (4)
	TP	−0.37% (2)	−2.39% (2)	−3.56% (2)	−1.82% (3)	−1.33% (4)
	$L/(at)^{1/2}$	44.72	70.71	100	141.4	223.6
	Flügge	1.7423 (2)	2.9693 (3)	4.4274 (3)	6.1915 (4)	10.0209 (5)
	SAP 2000	1.7384 (2)	2.9672 (3)	4.4266 (3)	6.1920 (4)	10.0234 (5)
5	WS	−22.4% (2)	−13.6% (3)	−9.31% (3)	−6.53% (4)	−4.05% (5)
	CK	−10.7% (2)	−1.76% (3)	−6.22% (3)	−2.87% (4)	−2.80% (5)
	TP	−1.29% (2)	−0.71% (3)	−2.22% (3)	−1.72% (4)	−2.03% (5)
	$L/(at)^{1/2}$	22.36	35.35	50	70.71	111.8
	Flügge	4.7968 (3)	7.8453 (4)	11.2271 (5)	16.0856 (6)	25.6822 (8)
	SAP 2000	4.7860 (3)	7.8413 (4)	11.2272 (5)	16.0912 (6)	25.6942 (8)
2	WS	−9.94% (3)	−5.90% (4)	−3.99% (5)	−2.73% (6)	−1.66% (8)
	CK	−7.52% (4)	−6.32% (5)	−5.32% (5)	−4.42% (6)	−2.39% (8)
	TP	+2.63% (3)	+1.02% (4)	+0.18% (5)	−0.58% (6)	−1.00% (8)
	$L/(at)^{1/2}$	8.944	14.14	20	28.28	44.72
	Flügge	9.9245 (4)	16.2594 (6)	22.8521 (7)	32.7534 (8)	51.7147 (11)
	SAP 2000	9.9065 (4)	16.2453 (6)	22.8544 (7)	32.7937 (8)	51.7631 (11)
1	WS	−5.08% (4)	−3.04% (6)	−2.12% (7)	−1.47% (8)	−0.87% (11)
	CK	−3.79% (5)	−3.31% (6)	−3.54% (8)	−1.88% (9)	−3.05% (11)
	TP	+7.24% (4)	+4.73% (6)	+2.78% (7)	+1.25% (8)	+0.20% (11)
	$L/(at)^{1/2}$	4.472	7.071	10	14.14	22.36

C/C, C/H, and C/F cylindrical shells, respectively. For H/H shells, there appears to be no pattern to which one can set limits on the CK formula.

5. The TP formula is in excellent agreement with the Flügge theory (within 5% absolute relative error) for asymmetric modes of deformation ($n^* > 0$), provided that, $\lambda \geqslant 10$, 8, 6, and 2, for C/C, C/H, H/H, and C/F cylindrical shells, respectively.
6. For H/F and F/F cylindrical shells, the WS formula is not recommended for estimating the inextensional natural frequency of the shell, corresponding to $n = 2$. The CK and TP

predictions for F/F cylindrical shells are identical to the analytical solution of Rayleigh. On the other hand, for H/F cylindrical shells, the CK and TP predictions are in excellent agreement with the analytical solution (within 5% absolute relative error) for $L/a \geqslant 2.8$ and $\geqslant 1.2$, respectively.

Appendix A. Nomenclature

a	mean radius of cylindrical shell
C_S, C_P	constants given in Table 1
D	flexural rigidity ($= Et^3/12(1-\nu^2)$)
E	Young's modulus of elasticity
G	shear modulus of elasticity ($= E/2(1+\nu)$)
I	second moment of area of cross-section
K	$= (12(1-\nu^2))^{1/4}$
L	axial length of shell
$L_1, \ldots, L_6$	partial differential operators defined by Eq. (2)
n	circumferential modenumber
n^*	circumferential modenumber associated with the fundamental mode
t	thickness of shell
u, v, w	axial, circumferential and radial components of displacement, respectively
U, V, W	θ-independent complex amplitudes of the displacement components, Eq. (4)
x	axial-length co-ordinate of shell
y	characteristic Bernoulli–Euler beam functions
z	normal-length co-ordinate of shell (positive outwards)
BC	boundary conditions
C	clamped edge of shell (held circular and plane)
CK	Calladine–Koga formula for the natural frequency of shell, Eq. (11)
F	free edge of shell
FE	finite-element method
H	freely supported edge of shell (held circular but unrestrained axially)
LW	long wave
SW	short wave
TP	Timoshenko beam mounted on Pasternak foundation
WS	Weingarten–Soedel formula for natural frequency of shell, Eq. (6)
β	dimensionless frequency parameter for Bernoulli–Euler beam ($= \omega L^2\sqrt{\rho A/EI}$)
λ	non-dimensional length of shell ($= L/(at)^{1/2}$)
Λ	non-dimensional length of shell ($= Lt^{1/2}/a^{3/2}$)
Δ	non-dimensional frequency parameter ($= \omega a(\rho(1-\nu^2)/E)^{1/2}$)
Ω	non-dimensional frequency parameter ($= \omega(a^2/t)(\rho(1-\nu^2)/E)^{1/2}$)
Δ^*	"fundamental" non-dimensional frequency parameter
Ω^*	"fundamental" non-dimensional frequency parameter
ν	Poisson's ratio
θ	circumferential co-ordinate (in radians)

ρ	mass density
τ	time
ω	circular natural frequency of vibration
$\nabla^4(..)$	bi-harmonic operator, $= \partial^4/\partial x^4(\ldots) + 2\partial^4/\partial x^2\partial\theta^2(\ldots) + \partial^4/\partial\theta^4(\ldots)$, $\nabla^8 \equiv \nabla^4(\nabla^4)$
$(\ldots)'$	$\mathrm{d}(\ldots)/\mathrm{d}x$

References

[1] A.E.H. Love, On the small free vibrations and deformations of thin elastic shells, Philosophical Transactions of the Royal Society of London 179A (1888) 456–491.
[2] A.W. Leissa, Vibration of shells, NASA SP-228, 1973.
[3] W.T. Koiter, A consistent first approximation in the general theory of thin elastic shells, Proceedings of the First IUTAM Symposium, 1960, pp. 12–33.
[4] K. Forsberg, Influence of boundary conditions on the modal characteristics of thin cylindrical shells, Journal of the American Institute of Aeronautics and Astronautics 2 (1964) 2150–2157.
[5] G.B. Warburton, Vibration of thin cylindrical shells, Journal of Mechanical Sciences 7 (1965) 399–407.
[6] R.N. Arnold, G.B. Warburton, Flexural vibrations of walls of thin cylindrical shells having freely supported ends, Proceedings of the Royal Society of London A197 (1949) 238–256.
[7] H. Kraus, Thin Elastic Shells, Wiley, New York, 1967.
[8] J.H. Percy, T.H.H. Pian, S. Klein, D.R. Navaratna, Application of matrix displacement method to linear elastic analysis of shells of revolution, Journal of the American Institute of Aeronautics and Astronautics 3 (1965) 2138–2145.
[9] Y.Y. Yu, Free vibrations of thin cylindrical shells having finite lengths with freely supported and clamped edges, Journal of Applied Mechanics 22 (1955) 547–552.
[10] V.I. Weingarten, Free vibration of thin cylindrical shells, Journal of the American Institute of Aeronautics and Astronautics 2 (1964) 717–722.
[11] W. Soedel, A new frequency formula for closed circular cylindrical shells for a large variety of boundary conditions, Journal of Sound and Vibration 70 (1980) 209–217.
[12] C.R. Calladine, Theory of Thin Shells, Cambridge University Press, Cambridge, 1983.
[13] T. Koga, Effects of boundary conditions on the free vibrations of circular cylindrical shells, Journal of the American Institute of Aeronautics and Astronautics 26 (1988) 1387–1394.
[14] M. El-Mously, A Timoshenko-beam-on-Pasternak-foundation analogy for cylindrical shells, Journal of Sound and Vibration 261 (2003) 635–652.
[15] W. Flügge, Stresses in Shells, Springer, Berlin, 1960.
[16] M. El-Mously, Free Vibration of Cylindrical and Hyperboloidal Cooling-tower Shells, Ph.D. Dissertation, University of Cambridge, 1997.
[17] M. El-Mously, Fundamental frequencies of Timoshenko beams mounted on Pasternak foundation, Journal of Sound and Vibration 228 (1999) 452–457.